



# Validation of carbon isotope fractionation in algal lipids as a $p\text{CO}_2$ proxy using a natural $\text{CO}_2$ seep (Shikine Island, Japan)

Caitlyn R. Witkowski<sup>1,a</sup>, Sylvain Agostini<sup>2</sup>, Ben P. Harvey<sup>2</sup>, Marcel T. J. van der Meer<sup>1</sup>, Jaap S. Sinninghe Damsté<sup>1,3</sup>, and Stefan Schouten<sup>1,3</sup>

<sup>1</sup>Department of Marine Microbiology and Biogeochemistry, Royal Netherlands Institute for Sea Research, Den Burg (Texel), 1790AB, and Utrecht University, the Netherlands

<sup>2</sup>Shimoda Marine Research Center, University of Tsukuba, Shimoda, 415-0025, Japan

<sup>3</sup>Department of Geosciences, Utrecht University, Utrecht, 3508 TA, the Netherlands

<sup>a</sup>present address: School of Earth Sciences, University of Bristol, Bristol, UK

**Correspondence:** Caitlyn R. Witkowski (caitlyn.witkowski@bristol.ac.uk)

Received: 26 April 2019 – Discussion started: 3 May 2019

Revised: 25 September 2019 – Accepted: 15 October 2019 – Published: 25 November 2019

**Abstract.** Carbon dioxide concentrations in the atmosphere play an integral role in many Earth system dynamics, including its influence on global temperature. The past can provide insights into these dynamics, but unfortunately reconstructing long-term trends of atmospheric carbon dioxide (expressed in partial pressure;  $p\text{CO}_2$ ) remains a challenge in paleoclimatology. One promising approach for reconstructing past  $p\text{CO}_2$  utilizes the isotopic fractionation associated with  $\text{CO}_2$  fixation during photosynthesis into organic matter ( $\varepsilon_p$ ). Previous studies have focused primarily on testing estimates of  $\varepsilon_p$  derived from the  $\delta^{13}\text{C}$  of species-specific alkenone compounds in laboratory cultures and mesocosm experiments. Here, we analyze  $\varepsilon_p$  derived from the  $\delta^{13}\text{C}$  of more general algal biomarkers, i.e., compounds derived from a multitude of species from sites near a  $\text{CO}_2$  seep off the coast of Shikine Island (Japan), a natural environment with  $\text{CO}_2$  concentrations ranging from ambient (ca.  $310\ \mu\text{atm}$ ) to elevated (ca.  $770\ \mu\text{atm}$ )  $p\text{CO}_2$ . We observed strong, consistent  $\delta^{13}\text{C}$  shifts in several algal biomarkers from a variety of sample matrices over the steep  $\text{CO}_2$  gradient. Of the three general algal biomarkers explored here, namely loliolide, phytol, and cholesterol,  $\varepsilon_p$  positively correlates with  $p\text{CO}_2$ , in agreement with  $\varepsilon_p$  theory and previous culture studies.  $p\text{CO}_2$  reconstructed from the  $\varepsilon_p$  of general algal biomarkers show the same trends throughout, as well as the correct control values, but with lower absolute reconstructed values than the measured values at the elevated  $p\text{CO}_2$  sites. Our results show that naturally occurring  $\text{CO}_2$  seeps may provide useful testing

grounds for  $p\text{CO}_2$  proxies and that general algal biomarkers show promise for reconstructing past  $p\text{CO}_2$ .

## 1 Introduction

The current increase in the atmospheric concentration of carbon dioxide (expressed in partial pressure,  $p\text{CO}_2$ ) plays a leading role in climate change (Forster et al., 2007).  $p\text{CO}_2$  is significantly higher now than it has been in the past 800 ka (Lüthi et al., 2008), and although long-term changes in  $p\text{CO}_2$  are not uncommon over millions of years (Foster et al., 2017), this current spike in  $p\text{CO}_2$  has occurred within only the past 2 centuries (IPCC, 2013). Uncertainties remain on the exact magnitude to which  $p\text{CO}_2$  influences climate, as well as the exact response of the environment to these climate changes. Long-term  $p\text{CO}_2$  trends help us better understand the context for these changes and are reconstructed via indirect means, i.e., environmental proxies. Two proxies can span timescales over 100 Ma (Foster et al., 2017), e.g., the terrestrial paleosol proxies and leaf stomata. The paleosol proxy has large uncertainties due to the difficulties in constraining soil respiration (Breecker et al., 2010; Cotton and Sheldon, 2012) due to carbon isotopic fractionation during microbial decomposition (Bowen and Beerling, 2004), carbonate diagenesis (Quast et al., 2006), and other local and regional influences on carbon cycles in these terrestrial settings. Although the leaf stomata proxy is often better constrained than

paleosols, some experiments do not show the expected trends (Ellsworth et al., 2011; Ward et al., 2013; DaMatta et al., 2016), suggesting that factors other than  $p\text{CO}_2$ , e.g., ecological systems, species, and development stage, also impact the leaf stomata proxy (Xu et al., 2016). The development of new proxies for  $p\text{CO}_2$  may help us better constrain past long-term trends, particularly marine-based proxies, which tend to have more homogenized signals but are currently relatively limited in time.

A proxy that has been explored with mixed success over the past several decades is the stable carbon isotopic fractionation associated with photosynthetic inorganic carbon fixations ( $\varepsilon_p$ ), which has been shown to positively correlate with  $p\text{CO}_2$  (Bidigare et al., 1997; Jasper and Hayes, 1990; Zhang et al., 2013).  $\varepsilon_p$  occurs as the  $\text{CO}_2$ -fixing enzyme in photoautotrophs, rubisco (ribulose 1,5-biphosphate carboxylase oxygenase), favors  $^{12}\text{C}$ , which consequently results in photosynthates isotopically more depleted in  $^{13}\text{C}$  than the original carbon source. A greater abundance of  $\text{CO}_2$  increases rubisco-based isotopic discrimination, resulting in an even lower  $^{13}\text{C}/^{12}\text{C}$  ratio ( $\delta^{13}\text{C}$ ) in photoautotroph biomass (Farquhar et al., 1982, 1989; Francois et al., 1993; Popp et al., 1989). When this phototrophic biomass is preserved in the geologic record, the  $\delta^{13}\text{C}$  of sedimentary organic matter can be used to reconstruct  $p\text{CO}_2$  (Hayes et al., 1999). The largely mixed contributions and diagenetic processes on bulk organic matter can, however, mask this signal (Hayes, 1993; Hayes et al., 1999). Thus, isotope analysis of specific biomarker lipids is preferred in order to better define the source of the  $\delta^{13}\text{C}$  signal (Jasper and Hayes, 1990; Pagani, 2002).

The most studied biomarkers for calculating  $\varepsilon_p$  are alkenones, i.e., long-chain unsaturated methyl and ethyl ketones produced by select haptophytes (Volkman et al., 1980; de Leeuw et al., 1980). The stable carbon isotopic fractionation of alkenones has been studied using cultures and mesocosms with controlled environments (Laws et al., 1995; Benthien et al., 2007), but conditions do not always mimic natural environments and the natural variation in carbonate chemistry that occurs on a daily to seasonal timescales. Furthermore, these experiments are also time-consuming given that they must have delicately balanced water chemistry, including  $\text{CO}_2$ [aq] concentrations, pH, and alkalinity, as well as nutrients such as nitrate and phosphate (Popp et al., 1998; Laws et al., 1995; Bidigare et al., 1997), along with the additional challenge of maintaining a constant  $\delta^{13}\text{C}$  of the  $\text{CO}_2$ [aq], while photoautotrophs continually enrich the growth water as they fix  $\text{CO}_2$ . Water column studies (Bidigare et al., 1997) and surface sediments (Pagani, 2002) have been applied but rarely reach elevated  $p\text{CO}_2$  levels like those encountered in the past.

Here we use an alternative approach by analyzing algal lipids near natural  $\text{CO}_2$  seep systems. In tectonically active zones, volcanically induced seeps consistently bubble high  $p\text{CO}_2$  concentrations into the surrounding water, substantially increasing the local  $\text{CO}_2$  concentrations in the wa-

ter and providing an environment referent to past and future high- $\text{CO}_2$  worlds.  $\text{CO}_2$  seeps were previously overlooked for biological studies due to the typically high sulfide ( $\text{H}_2\text{S}$ ) concentrations associated with volcanic degassing that make these environments largely uninhabitable (Dando et al., 1999). However, certain  $\text{CO}_2$  seep systems have been found to have low  $\text{H}_2\text{S}$  concentrations, making them suitable for ocean acidification experiments (Hall-Spencer et al., 2008), prompting further research in, e.g., the Mediterranean (Boatta et al., 2013), Japan (Agostini et al., 2015), Papua New Guinea (Fabricius et al., 2011), and New Zealand (Brinkman and Smith, 2015). These sites may provide an ideal testing ground for the impact of isotopic fractionation on algal lipids where environmental conditions are at naturally balanced levels with the exception of the large gradient of  $\text{CO}_2$  concentrations.

In our study, we explore the relationship between  $\varepsilon_p$  and  $\text{CO}_2$ [aq] across several preestablished sites, with different (temporally consistent) levels of  $p\text{CO}_2$  at the warm, temperate  $\text{CO}_2$  seep in Mikama Bay, offshore of Shikine Island, Japan. We test this relationship using general algal biomarkers, i.e., compounds derived from a multitude of species and have rarely been used for  $\varepsilon_p$ -based  $p\text{CO}_2$  reconstructions despite their potential utility (Witkowski et al., 2018; Popp et al., 1989; Freeman and Hayes, 1992).

## 2 Materials and methods

### 2.1 Sample site

The site is briefly described here. For further details, we refer to Agostini et al. (2018). Mikama Bay is located on the south-southwest corner of Shikine Island, offshore of the Izu Peninsula, Japan ( $34.320865^\circ\text{N}$ ,  $139.204868^\circ\text{E}$ ), and has several venting locations in the north of the bay (Fig. 1). The gas emitted from the seep contains 98%  $\text{CO}_2$ , and the bay has a spatially and temporally constant total alkalinity averaging at  $2265 \pm 10 \mu\text{mol kg}^{-1}$ . Samples were collected from three preestablished  $p\text{CO}_2$  sites (Agostini et al., 2015), a “control  $p\text{CO}_2$ ” site in an adjacent bay outside the influence of the  $\text{CO}_2$  seep ( $p\text{CO}_2$   $309 \pm 46 \mu\text{atm}$ ), a “mid- $p\text{CO}_2$ ” site ( $p\text{CO}_2$  ca.  $460 \pm 40 \mu\text{atm}$ ), and a “high- $p\text{CO}_2$ ” site ( $p\text{CO}_2$   $769 \pm 225$ ) (Fig. 1).  $p\text{CO}_2$  estimates are based on the carbonate chemistry parameters ( $\text{pH}_{\text{NBS}}$ , temperature, salinity, and total alkalinity) of water in the bay and calculated using the program  $\text{CO}_2\text{sys}$  (Agostini et al., 2018; Harvey et al., 2018). Temperature (annual range ca.  $14$  to  $28^\circ\text{C}$ ) and salinity (ca.  $34\text{‰}$ ) are relatively homogenous throughout the bay and do not differ between the elevated  $p\text{CO}_2$  sites and control  $p\text{CO}_2$  sites (Agostini et al. 2018). Currents and wind were measured in October 2014 and April 2015 (Agostini et al., 2015). October 2014 measurements showed moderate turbulent winds (ranging from  $0.6$  to  $11.5 \text{ m s}^{-1}$ , with an average of  $4.5 \text{ m s}^{-1}$ ) associated with current velocities (ranging

from 0 to 1.6 knots, average 0.4 knots) at 5 m in the surface water, whereas April 2015 measurements showed moderate north-northeast winds ( $1.5\text{--}8.6\text{ m s}^{-1}$ , average  $5.1\text{ m s}^{-1}$ ) associated with low current velocities (0–0.2 knots, average 0.04 knots). Monthly surveys in the bay over the past 5 years show that these sites have similar annual mean values for temperature, salinity, and currents. Weather station data show that the severity of seasonal extreme weather event (e.g., typhoons) varies on an annual basis (Japan Meteorological Agency, <https://www.jma.go.jp/en/typh/>, last access: 1 April 2019).

## 2.2 Materials

Samples were collected in June and September of 2016 (indicated in Fig. 1). All samples were collected in at least triplicate for each site (control  $p\text{CO}_2$ , mid- $p\text{CO}_2$  and high- $p\text{CO}_2$  site). Additional control sites (ca. 1.8 and 2.4 km away from the  $\text{CO}_2$  seep) around the island were taken to ensure the fidelity of the control site closest to the seep. June sampling included surface waters for dissolved inorganic carbon (DIC) measurements, surface sediments, and benthic diatoms attached to surface sediment through extracellular polymeric substance production. In September, macroalgae and plankton tows were collected, in addition to surfaced water DIC and surface sediments, taken in triplicate at each site on four separate days.

Water for the  $\delta^{13}\text{C}$  of DIC analysis was collected by overfilling glass vials with sea surface water and adding mercury chloride (0.5 %) before closing with a septa cap and sealing with electrical tape. Surface sediments were collected by divers using geochemical sample bags. Macroalgae and benthic diatoms were scraped off submerged rocks at each respective site. A  $25\text{ }\mu\text{m}$  mesh plankton net (“small plankton net”, Rigo, Saitama, Japan) was towed 50 m three times per site and filtered using a portable hand aspirator on the boat over a single  $0.7\text{ }\mu\text{m}$  GF/F (glass fiber filter; combusted prior to sampling for 4 h at  $450\text{ }^\circ\text{C}$ ). All samples were immediately frozen; once back in the lab, these were freeze-dried and kept in a refrigerator.

## 2.3 Methods

Each seawater sample was measured for the  $\delta^{13}\text{C}$  of DIC in duplicate on a Thermo Scientific Gas Bench II coupled to a Thermo Scientific Delta V mass spectrometer. Prior to running samples, 12 mL vials were prepared with  $100\text{ }\mu\text{L}$  of 85 %  $\text{H}_3\text{PO}_4$  and flushed with He. A total of  $500\text{ }\mu\text{L}$  of seawater was added and left to react for at least 1 h prior to measuring the headspace. Standards were run at the start, end, and every six runs of a sequence. Standards were prepared with 0.3 mg of  $\text{Na}_2\text{CO}_3$  and 0.4 mg of  $\text{Ca}_2\text{CO}_3$  (all calibrated against NBS-19) flushed with He, injected with  $500\text{ }\mu\text{L}$  of 85 %  $\text{H}_3\text{PO}_4$ , and reacted for 1 h. The headspace was measured, and average values and standard deviation er-

rors reported are based on 6 measurements for June (3 at the high- $p\text{CO}_2$  site and 3 at the control) and 36 measurements for September (3 each at the high- $p\text{CO}_2$  site, mid- $p\text{CO}_2$  site, and control, collected on four separate days).

Freeze-dried sediments, benthic diatoms, and macroalgae were homogenized using mortar and pestle and extracted using a Dionex 250 accelerated solvent extractor at  $100\text{ }^\circ\text{C}$ ,  $7.6 \times 106\text{ Pa}$  using dichloromethane (DCM):MeOH (9 : 1  $v/v$ ). GF/Fs containing plankton net material were cut into  $1\text{ mm} \times 1\text{ mm}$  squares and extracted using ultrasonication ( $5\times$ ) with 2 mL dichloromethane (DCM):MeOH (9 : 1  $v/v$ ). All total lipid extracts (TLEs) were hydrolyzed by refluxing the TLE with 1 N of KOH in MeOH for 1 h and neutralized to pH 5 using 2 N of HCl in MeOH. Bi-distilled water (2 mL) and DCM (2 mL) was added ( $5\times$ ) to the hydrolyzed centrifuge tubes and the organic matter in the DCM layers were pooled and dried over  $\text{Na}_2\text{SO}_4$ . The resulting hydrolyzed TLEs were eluted over an alumina packed column and separated into apolar (hexane:DCM, 9 : 1  $v/v$ ), ketone (DCM), and polar (DCM:MeOH, 1 : 1  $v/v$ ) fractions. Polar fractions were silylated using pyridine:N,O-Bis(trimethylsilyl)trifluoroacetamide (BSTFA) (1 : 1  $v/v$ ) and heated at  $60\text{ }^\circ\text{C}$  for 1 h prior to analyses on the gas chromatography-flame ionization detector (GC-FID), gas chromatography-mass spectrometry (GC-MS), and gas chromatography isotope-ratio mass spectrometry (GC-IRMS).

Silylated polar fractions were analyzed by GC-FID for quantification. Based on the quantities, fractions were diluted with ethyl acetate and ca.  $1\text{ }\mu\text{g}$  of polar fraction was injected on-column for GC-MS to identify compounds and for GC-IRMS to measure the isotopic composition of specific compounds. Each instrument is equipped with the same CP-Sil 5 column ( $25\text{ m} \times 0.32\text{ mm}$ ;  $d_f 0.12\text{ }\mu\text{m}$ ) and He is used as carrier gas. GC oven was programmed from  $70\text{ }^\circ\text{C}$  to  $130\text{ }^\circ\text{C}$  at  $20\text{ }^\circ\text{C min}^{-1}$  and then to  $320\text{ }^\circ\text{C}$  at  $4\text{ }^\circ\text{C min}^{-1}$ , which was held for 10 min. All three instruments use the same in-house mixture of  $n$ -alkanes and fatty acids to check chromatography performance at the start of each day (GC-standard). For compound-specific stable carbon isotope analysis using GC-IRMS, additional standards with known isotopic values ( $-32.7\text{ }‰$  and  $-27.0\text{ }‰$ ) of per deuterated (99.1 %)  $n$ -alkanes ( $\text{C}_{20}$  and  $\text{C}_{24}$ , respectively), were co-injected with the GC-standard. Samples were also co-injected with the same GC-IRMS standards to monitor instrument performance. Every day, the Isolink II combustion reactor of the GC-IRMS was oxidized for at least 10 min, backflushed with He for 10 min, and purged for 5 min; a shorter version of this sequence is conducted in post-sample seed oxidation, which includes 2 min oxidation, 2 min He backflush, and a 2 min purge conditioning line. Longer oxidations were run weekly. Each derivatized compound was corrected for the  $\delta^{13}\text{C}$  of the BSTFA used in silylation ( $-32.2\text{ }‰$ ).

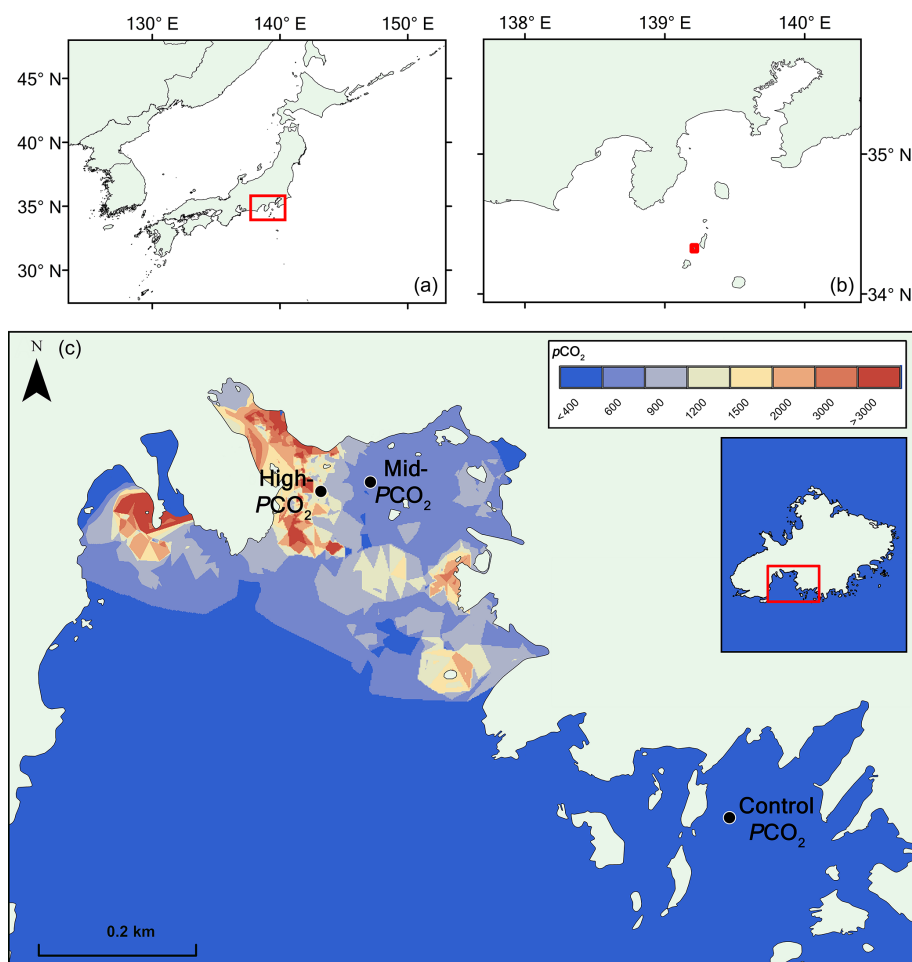


**Figure 1.** Map of  $p\text{CO}_2$  in the study region at Shikine Island (Japan). Panels (a, b) show the geographical context. Panel (c) shows the bay on Shikine Island, with spatial variability in  $p\text{CO}_2$  (Agostini et al., 2018), computed using the nearest neighbor algorithm in ArcGIS 10.2 software (<http://www.esri.com/software/arcgis/>, last access: 1 November 2018).

### 3 Results

Samples from the different matrices were collected at several control  $p\text{CO}_2$  sites ( $309 \pm 46$ ), at a mid- $p\text{CO}_2$  site (ca. 100 m from the venting area;  $460 \pm 40 \mu\text{atm}$ ), and near the venting area (high- $p\text{CO}_2$  site;  $769 \pm 225 \mu\text{atm}$ ) during June and September 2016 (Fig. 1), which included June-collected surface waters (for DIC), surface sediments, and benthic diatoms and September-collected surface waters (for DIC), surface sediments, plankton net tows, and macroalgae.

The  $\delta^{13}\text{C}$  of DIC demonstrated minimal change over the gradient of  $\text{CO}_2$  and minimal change between the two seasons (Table S1 in the Supplement). The June  $\delta^{13}\text{C}$  of DIC was  $0.2 \pm 0.2 \text{‰}$  ( $\pm\text{SD}$ ;  $N = 3$ ) at the control site and  $0.5 \pm 0.04 \text{‰}$  ( $N = 3$ ) at the high- $p\text{CO}_2$  site. The September  $\delta^{13}\text{C}$  of DIC was  $-0.4 \pm 0.2 \text{‰}$  ( $N = 8$ ) at the control site,  $-0.1 \pm 0.1 \text{‰}$  ( $N = 8$ ) at the mid- $p\text{CO}_2$  site, and  $0.2 \pm 0.4 \text{‰}$  ( $N = 8$ ) at the high- $p\text{CO}_2$  site.

The polar fractions of the extracts of the surface sediments, plankton, macroalgae, and benthic diatoms showed a similar suite of compounds, observed across all sites and during both seasons. The most prominent compounds were loliolide, phytol,  $\text{C}_{14}$ – $\text{C}_{16}$  alkanols, and sterols, such as cholesta-5,22E-dien-3 $\beta$ -ol, cholesterol, 23-methylcholesta-5,22dienol, campesterol, stigmasterol, and  $\beta$ -sitosterol (e.g., Fig. 2). Terrestrial biomarkers, such as long-chain alcohols and triterpenoids were not detected. Loliolide, phytol, and cholesterol were targeted for stable carbon isotope analysis as the most abundant general algal biomarkers and with relatively good separation in the GC. The biological sources of these compounds will be discussed in Sect. 4.1.

Among the sample matrices, the  $\delta^{13}\text{C}$  of loliolide ranges from  $-19.8 \text{‰}$  to  $-22.0 \text{‰}$  at the control sites, from  $-20.5 \text{‰}$  to  $-22.9 \text{‰}$  at the mid- $p\text{CO}_2$  site, and from  $-23.1 \text{‰}$  to  $-29.0 \text{‰}$  at the high- $p\text{CO}_2$  site (Fig. 3a; Table S1). The  $\delta^{13}\text{C}$  of loliolide from June surface sediments shows the strongest change from the control site to the

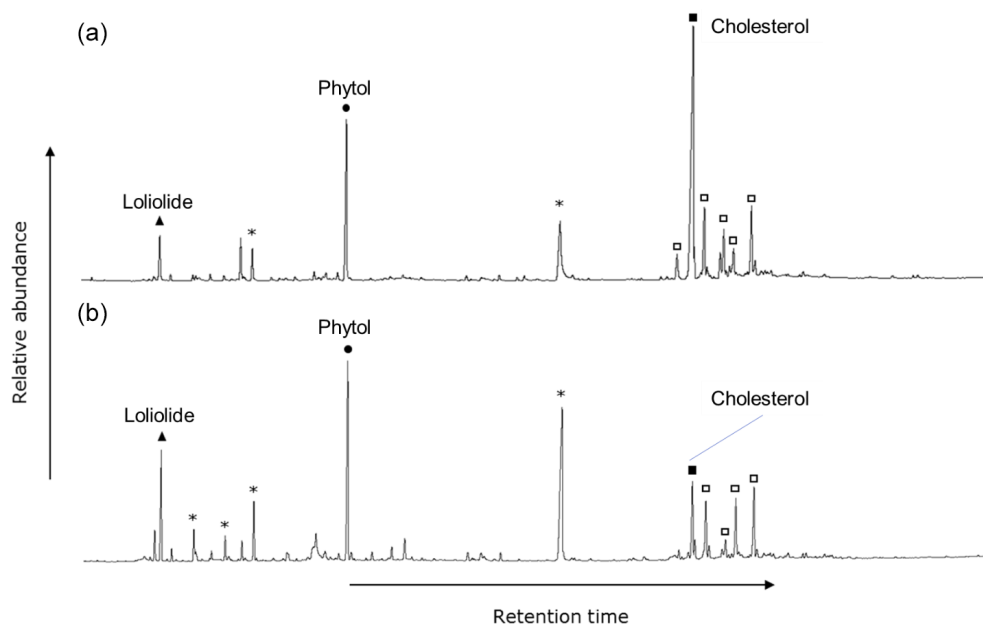


**Figure 2.** GC-FID trace of silylated polar fraction. June sediment collected at the (a) control site and (b) CO<sub>2</sub> vent, showing saturated fatty alcohols (asterisks) and sterols (squares), and the representative compounds found among all sample matrices, seasons, and CO<sub>2</sub> concentrations: loliolide, phytol, and cholesterol.

high-*p*CO<sub>2</sub> site (−21.2‰ to −29.0‰), followed by the δ<sup>13</sup>C of loliolide from September macroalgae (−21.3‰ to −25.7‰). A lesser δ<sup>13</sup>C shift is observed in the September surface sediment-derived loliolide (−19.8‰ to −23.1‰). The δ<sup>13</sup>C of the benthic diatom-derived loliolide (−20.2‰ to 23.6‰) and the plankton tow-derived loliolide show the smallest shifts from the control site to the high-*p*CO<sub>2</sub> site (−22.0‰ to −23.6‰).

Similar to the results of the δ<sup>13</sup>C of loliolide, the δ<sup>13</sup>C of phytol also consistently shows higher δ<sup>13</sup>C values in the control sites and lower δ<sup>13</sup>C values in the elevated *p*CO<sub>2</sub> sites among all samples types collected in both seasons (Fig. 3b; Table S2). For the whole sample set, the δ<sup>13</sup>C of phytol ranges from −18.9‰ to −22.6‰ at the control site, from −19.4‰ to −22.4‰ at the mid-*p*CO<sub>2</sub> site, and from −22.6‰ to −27.8‰ at the high-*p*CO<sub>2</sub> site (Fig. 3b), similar ranges to those observed for loliolide. A similar shift in δ<sup>13</sup>C values of phytol is observed with increasing *p*CO<sub>2</sub> in the June surface sediments (−22.6‰ to −27.8‰), the June benthic diatoms (−18.9‰ to −24.4‰), and the September macroalgae (−21.5‰ to −26.9‰). Smaller changes in the δ<sup>13</sup>C of phytol are observed for September plankton (−21.7‰ to −24.4‰) and September sediment (−20.5‰ to −22.6‰).

The δ<sup>13</sup>C of cholesterol likewise shows a similar trend to the other two biomarkers but with a smaller shift in the δ<sup>13</sup>C values from the control *p*CO<sub>2</sub> sites to the elevated *p*CO<sub>2</sub> sites. Among the different sample matrices, the δ<sup>13</sup>C of cholesterol ranges from −21.2‰ to −25.1‰ at the control site, −22.1‰ to −23.4‰ at the mid-*p*CO<sub>2</sub> site, and

−23.1‰ to −27.4‰ at the high-*p*CO<sub>2</sub> site (Fig. 3c; Table S1). The strongest change in the δ<sup>13</sup>C of cholesterol with increased *p*CO<sub>2</sub> occurs in the June surface sediments from −22.6‰ in the control to −27.8‰ at the high-*p*CO<sub>2</sub> site. The June benthic diatoms also have a large isotopic shift in the δ<sup>13</sup>C of cholesterol (−21.2‰ to −25.8‰), as does the September macroalgae (−22.7‰ to −25.8‰). The September surface sediments (−22.2‰ to −23.1‰) and plankton tow-derived cholesterol (−25.1‰ to −26.7‰), however, have a smaller shift from the control to the elevated *p*CO<sub>2</sub> sites.

## 4 Discussion

### 4.1 The δ<sup>13</sup>C differences in biomarkers among matrices and seasons

All three biomarkers, phytol, loliolide, and cholesterol, show a negative shift in δ<sup>13</sup>C values with increasing *p*CO<sub>2</sub> in each matrix and each season (Fig. 3), agreeing with the theory that higher *p*CO<sub>2</sub> conditions result in lower δ<sup>13</sup>C values in biomass (Farquhar et al., 1982). However, despite all having algal sources, the absolute isotope values vary for (1) each compound, (2) each matrix, and (3) both seasons, which we will now discuss.

First, the absolute values of δ<sup>13</sup>C values vary among the three compounds. This may be expected given the different biosynthetic pathways leading to formation of each compound (Schouten et al., 1998), as well as the different

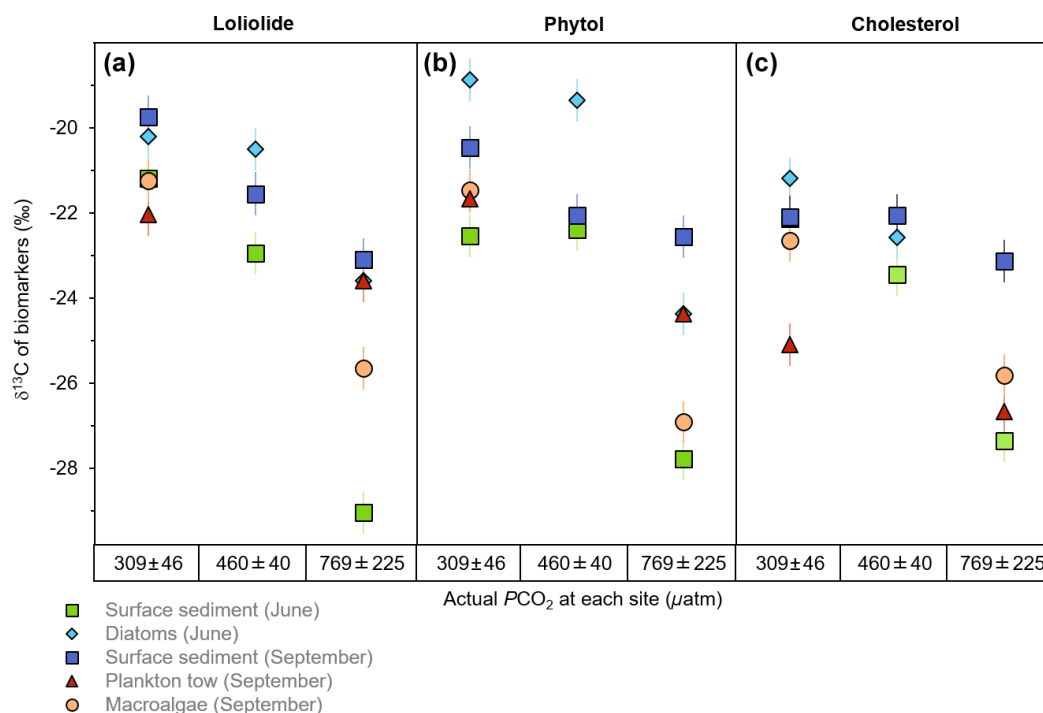


**Figure 3.** The  $\delta^{13}\text{C}$  of general algal biomarkers in sediments. (a) Loliolide, (b) phytol, and (c) cholesterol from the control, mid- $p\text{CO}_2$ , and high- $p\text{CO}_2$  sites during June and September from different sample matrices, including surface sediment (square), benthic diatoms (diamond), plankton tow (triangle), and macroalgae (circle).

contributors to each compound. Loliolide, considered a diatom biomarker in paleoreconstructions (e.g., Castañeda et al., 2009), is a diagenetic product of fucoxanthin (Repeta, 1989; Klok et al., 1984), a xanthophyll that contributes to approximately 10% of all carotenoids found in nature (Liaaen-Jensen, 1978). Phytol, considered a photoautotroph biomarker in paleoreconstructions (Hayes et al., 1990), is the side-chain of the vital and omnipresent pigment chlorophyll *a* that directly transfers sunlight energy into the photosynthetic pathway in nearly all photosynthetic organisms. Sterols, considered a general eukaryotic biomarker in paleoreconstructions, are the eukaryotic tetracyclic triterpenoid lipids used for critical regulatory roles of cellular functions, e.g., maintaining membrane fluidity (Nes et al., 1993). Although sterols are virtually restricted to eukaryotes, some exceptions have been found in bacteria (Wei et al., 2016). Here we only examine cholesterol, which is universally absent in prokaryotes and composes of up to 20%–40% of eukaryotic plasma membranes (Mouritsen and Zuckermann, 2004). Phytol and cholesterol may also have terrestrial sources, given that they are derived from all photoautotrophs and all eukaryotes, respectively. However, these samples were taken off the coast of a small island in the open ocean, and the absence of characteristic terrestrial biomarkers indicates that terrestrial contributions can be considered to be minimal. The close resemblance of the isotopic composition among all three compounds, including the primarily diatom-limited

compound loliolide, suggests that these compounds share relatively similar source organisms. Cholesterol shows a lessened isotopic shift compared to the other two compounds from the ambient to elevated  $p\text{CO}_2$  sites. Although we cannot fully exclude that this is due to terrestrial input, it is more likely due to the mobile eukaryotic zooplankton in the water column, which also contribute to the cholesterol signal.

Within the same biomarker and same season, some differences among matrices were observed. This difference may be due to the mobility of the matrix, as well as the algal assemblages. The plankton tow that captured free-floating surface water algae from that specific growth season is more readily transported by wind than the surface sediment, which likely reflects the culmination of multiple growth seasons throughout the water column. This is seen, for example, in the  $\delta^{13}\text{C}$  of cholesterol collected in September from the same control site where surface sediments are  $-22.2\text{‰}$  and plankton tows are  $-25.1\text{‰}$ , where the latter has possibly been transported from sites with elevated  $p\text{CO}_2$  levels. Similar differences among matrices are also observed in phytol and loliolide. The hypothesis of transportation affecting the isotopic signal in certain matrices is supported by the results from the macroalgae. The macroalgae, in contrast to the algae collected by plankton tows, were unaffected by transportation due to being fixed to the nearby rocks at each site. Thus, the isotopic composition of compounds of the macroalgae was similar to that of the surface sediments accumulated over a

long period, e.g.,  $-22.7\%$  for the  $\delta^{13}\text{C}$  of cholesterol at the September control site.

Finally, there is a difference in the  $\delta^{13}\text{C}$  values for biomarkers between seasons. The June-collected surface sediments and algae yielded a larger difference in  $\delta^{13}\text{C}$  values along the  $\text{CO}_2$  gradient than the September-collected surface sediments and algae. This seasonal difference may be due to extreme weather conditions experienced between the two sampling campaigns. Although typhoons are common in this region, in the weeks preceding the fieldwork in September, Shikine Island experienced an unusually high quantity of storms. The storms were also of unusual strength for this region of the Pacific, including typhoons Mindulle and Kompas, the severe tropical storms Omais and Chanthu, and the long-lived, erratic Lionrock typhoon. This atypical abundance and severity of storms observably ripped corals out of the rocks around Shikine Island and thus likely resuspended and transported some sediment around the bay. This would explain the reduced  $\delta^{13}\text{C}$  difference between the control and high- $p\text{CO}_2$  site in the surface sediments collected in September, as well as the readily transportable algae collected by the plankton tow, and would explain why the rock-affixed macroalgae, also collected in September, maintained a strong  $\delta^{13}\text{C}$  change across the transect.

#### 4.2 The $\varepsilon_p$ among general algal biomarkers

To further validate the impact of  $p\text{CO}_2$ , we calculated the isotopic fractionation of algal biomass based on the  $\delta^{13}\text{C}$  of the three biomarkers. Here we focus on surface sediments as they are a close analogue to the geological sediment records. Although the macroalgae and benthic diatoms also show strong isotopic fractionation, they represent a limited number of species and a single growth season. Furthermore, we calculated the  $\varepsilon_p$  from the June-collected surface sediments, which appear to be the least affected by typhoon activity and represent fractionation over multiple seasons.

To calculate  $\varepsilon_p$  in the June-collected surface sediments, we correct the  $\delta^{13}\text{C}$  of the organic matter ( $\delta_p$ ) for the  $\delta^{13}\text{C}$  of the inorganic carbon source for the producers of these compounds ( $\delta_d$ ) in Eq. (1):

$$\varepsilon_p = 1000 \cdot [(\delta_d + 1000) / (\delta_p + 1000) - 1]. \quad (1)$$

$\delta_p$  is calculated by correcting the  $\delta^{13}\text{C}$  for each individual biomarker for the offset with photosynthetic biomass caused by isotopic fractionation during biosynthesis. The isotopic offset between phytol and biomass is  $3.5 \pm 1.3\%$ , based on the average of 23 species compiled in Witkowski et al. (2018), and the isotopic offset between sterols and biomass is  $4.5 \pm 3.0\%$  based on the average of eight algal species (Schouten et al., 1998). The isotopic offset for loliolide from biomass, however, has not been determined. Because isoprenoids are formed from the same biosynthetic pathway, here we average the offset of the other two iso-

prenoids here ( $4.0\%$ ) to estimate a value for the difference between loliolide and biomass.

$\delta_d$  is calculated by correcting the measured  $\delta^{13}\text{C}$  of DIC for temperature (Mook, 1974) and pH (Madigan et al., 1989), which considers the relative contribution of different inorganic carbon species to the measured DIC. Based on the equations of Mook et al. (1974), we correct for the temperature-dependent carbon isotopic fractionation of dissolved  $\text{CO}_2$  with respect to  $\text{HCO}_3^-$  using the annual mean sea surface temperature for Shikine Island of  $20.4^\circ\text{C}$  (Agostini et al., 2018). Based on the equations of Madigan et al. (1989), we corrected for the  $\delta^{13}\text{C}$  of  $\text{HCO}_3^-$  and  $\delta^{13}\text{C}$  of  $\text{CO}_{2[\text{aq}]}$  mass balance calculation that accounts for the relative abundance of these inorganic carbon species based on pH (Lewis and Wallace, 1998) at the high- $p\text{CO}_2$  site ( $7.81 \text{ pH}_T$ ) and mid- $p\text{CO}_2$  site ( $7.99 \text{ pH}_T$ ), relative to the ambient control ( $8.14 \text{ pH}_T$ ). The corrected  $\delta_d$  values yield  $-10.1\%$  at the control site,  $-10.0\%$  at the mid- $p\text{CO}_2$  site, and  $-9.5\%$  at the high- $p\text{CO}_2$  site (Table S2).

$\varepsilon_p$  values consistently yield much higher values at the elevated  $p\text{CO}_2$  sites than the ambient control sites for all three biomarkers, which share similar trends and absolute values (Fig. 4; Table S3).  $\varepsilon_p$  derived from loliolide averages  $7.2 \pm 1.6\%$  at the control,  $9.2 \pm 1.6\%$  at the mid- $p\text{CO}_2$  site, and  $15.9 \pm 1.6\%$  at the high- $p\text{CO}_2$  site,  $\varepsilon_p$  derived from phytol at  $8.6 \pm 0.4\%$ ,  $8.6 \pm 0.9\%$ , and  $14.9 \pm 1.0\%$ , respectively, and  $\varepsilon_p$  derived from cholesterol at  $7.6 \pm 3.0\%$ ,  $9.2 \pm 3.1\%$ , to  $13.7 \pm 3.1\%$ , respectively, where errors represent the standard deviation of the triplicate samples taken at each site. These results show that  $\text{CO}_2$  has a profound impact on  $\varepsilon_p$  as it is the only variable with a large gradient in the bay. Given that maximum fractionation for algae species is ca.  $25\%$  to  $28\%$  in laboratory cultures (Goericke and Fry, 1994), the  $\text{CO}_2$  seep values suggests strong fractionation, but does not approach maximum fractionation ( $\varepsilon_f$ ) at the high- $\text{CO}_2$  site. This may be due to presence of carbon concentrating mechanism in phytoplankton, which utilize  $^{13}\text{C}$ -enriched bicarbonate, or possibly due to the presence of rubisco types with different  $\varepsilon_f$  values than previously assumed (Thomas et al., 2018).

#### 4.3 $p\text{CO}_2$ reconstructed from general algal biomarkers

We estimate  $p\text{CO}_2$  from the  $\varepsilon_p$  values, a relationship first derived for higher plants (Farquhar et al., 1982, 1989) and later adapted for algae (Jasper et al., 1994; Rau et al., 1996) in Eq. (2):

$$p\text{CO}_2 = [b / (\varepsilon_f - \varepsilon_p)] / K_0, \quad (2)$$

where  $\varepsilon_f$  reflects the maximum rubisco-based isotopic fractionation,  $b$  reflects species carbon demand per supply such as growth rate and cell-size (Jasper et al., 1994), and  $K_0$  reflects a constant to convert  $\text{CO}_{2[\text{aq}]}$  to  $p\text{CO}_2$  based on temperature and salinity (Weiss, 1974).  $\varepsilon_f$  for algal species range from  $25\%$  to  $28\%$  in laboratory cultures (Goericke and Fry,

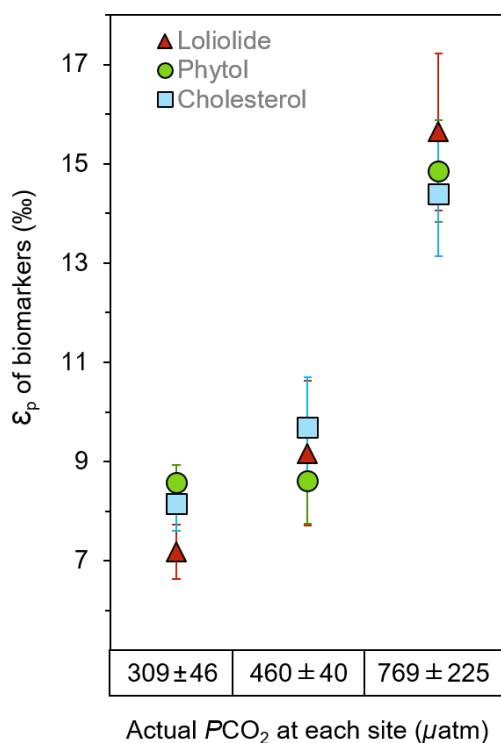


**Figure 4.** The  $\epsilon_p$  of general algal biomarkers in sediments. Loliolide (triangle), phytol (circle), and cholesterol (square) from the control, mid- $p\text{CO}_2$  and high- $p\text{CO}_2$  sites during June sediment collection.

1994); we use an average 26.5‰ with an uncertainty of 1.5‰ uniformly distributed for these general algal biomarkers (Witkowski et al., 2018). The  $b$  value is difficult to estimate as it is a catchall for factors other than  $p\text{CO}_2$  that affect fractionation and is particularly difficult to estimate for general algal biomarkers because they are derived from a multitude of species. Previous studies using phytol's diagenetic product phytane as a  $p\text{CO}_2$  proxy (Bice et al., 2006; Sinninghe Damsté et al., 2008; van Bentum et al., 2012) have used a mean value of  $170\text{‰ kg } \mu\text{M}^{-1}$ , similar to the mean of alkenone producers. This is supported by a compilation of the  $\delta^{13}\text{C}$  values of modern surface sediment organic matter mean average of  $168 \pm 43\text{‰ kg } \mu\text{M}^{-1}$  (Witkowski et al., 2018) and a single study on phytol in the equatorial Pacific Ocean (Bidigare et al., 1997). We apply this average, rounded to  $170 \pm 50\text{‰ kg } \mu\text{M}^{-1}$ , to all three general algal biomarkers.

The resulting reconstructed  $p\text{CO}_2$  estimations show the expected values in the control sites and much higher values in the elevated  $\text{CO}_2$  sites among all three biomarkers (Fig. 5; Table S3). Loliolide shows the biggest shift, from  $239 + 50 / - 49 \mu\text{atm}$  at the control,  $266 + 57 / - 54 \mu\text{atm}$  at mid- $p\text{CO}_2$  site, and  $437 + 113 / 96 \mu\text{atm}$  at the high- $p\text{CO}_2$  site. Phytol has a similar but slightly smaller shift in  $p\text{CO}_2$  estimates to loliolide, with estimations of  $264 + 55 / - 54$ ,  $291 + 56 / - 53$ , and  $444 + 98 / - 87 \mu\text{atm}$  at the control, mid- $p\text{CO}_2$  site, and high- $p\text{CO}_2$  sites, respectively. Cholesterol

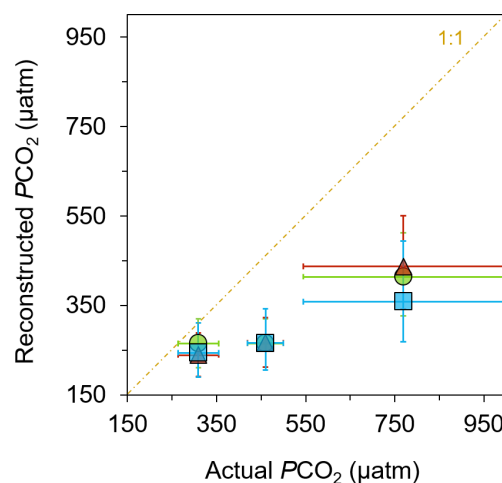


**Figure 5.** Reconstructed  $p\text{CO}_2$  from general algal biomarkers.  $p\text{CO}_2$  reconstructed from the  $\delta^{13}\text{C}$  of loliolide (triangle), phytol (circle), and cholesterol (square) in June-collected sediments versus the actual  $p\text{CO}_2$  measured at each location (Agostini et al., 2018; Harvey et al., 2018).

shifts in a similar manner to the other two biomarkers with  $244 + 67 / - 54$ ,  $266 + 77 / - 61$ , and  $358 + 136 / - 90 \mu\text{atm}$ , respectively. These reconstructed values closely match each other and trend in the same direction as the actual values.

The reconstructed  $p\text{CO}_2$  values derived from the  $\delta^{13}\text{C}$  of general algal biomarkers closely match the actual measured  $p\text{CO}_2$  values of the control (Fig. 5), i.e.,  $309 \pm 46 \mu\text{atm}$  (Agostini et al., 2018; Harvey et al., 2018), when considering the uncertainty in the reconstructed estimations. However, the proxies underestimate the absolute values measured at the elevated  $p\text{CO}_2$  sites (Fig. 5; Table S3), i.e.,  $460 \pm 40 \mu\text{atm}$  at the mid- $p\text{CO}_2$  site and  $769 \pm 225 \mu\text{atm}$  at the high- $p\text{CO}_2$  site (Agostini et al., 2018; Harvey et al., 2018). There are several possible explanations as to why there is an underestimation. As discussed above, carbonate concentration mechanisms may be operating in a large number of phytoplankton, such that they become relatively enriched in  $^{13}\text{C}$  and thus lead to lower reconstructed  $p\text{CO}_2$  values (Stoll et al., 2019; Badger et al., 2019). There is also a large uncertainty in the  $b$  value applied, which may be much lower than the value assumed here. However, if this is the case, then  $p\text{CO}_2$  values reconstructed for past times may be much higher, leading to considerable discrepancies with other  $p\text{CO}_2$  proxies (cf. Witkowski et al., 2018). A simple explanation for this underestimation may be some site limitations. The high variability of  $p\text{CO}_2$  at these sites could have impacted the reconstructed values, as these algae could have been exposed to much different, and perhaps lower, levels than those observed during the times that  $p\text{CO}_2$  values were measured. Furthermore, there is a strong possibility of allochthonous marine input of sediment at the mid- $p\text{CO}_2$  and high- $p\text{CO}_2$  sites, i.e., input from sediment outside of the bay area. This



allochthonous input seems likely given the intense weather conditions that occur annually in this small bay in which lateral transport of sediment could bring algal material grown in ambient  $p\text{CO}_2$  conditions into the bay and dampen the overall  $p\text{CO}_2$  signal picked up in the biomarkers. Future research conducted at another  $\text{CO}_2$  seep setting with different weather and current conditions could illuminate this.

## 5 Conclusions

We analyzed the  $\delta^{13}\text{C}$  of general algal biomarkers in surface sediments, plankton, benthic diatoms, and macroalgae collected in a transect from a  $\text{CO}_2$  vent during two seasons. The strong  $\delta^{13}\text{C}$  change between the control and elevated  $p\text{CO}_2$  sites suggest that the increased  $\text{CO}_2$  concentrations in the seawater does indeed influence fractionation of photoautotrophic biomass and validates previous  $p\text{CO}_2$  reconstructions, which have considered utilizing general algal biomarkers for this purpose. Reconstructions correctly estimate control values, though reconstructions at the elevated  $p\text{CO}_2$  sites show underestimations of the actual  $p\text{CO}_2$ , possibly due to the allochthonous input from nearby marine sediments deposited under normal  $p\text{CO}_2$  levels caused by the intense annual typhoon activity in this region. Our results show that  $\text{CO}_2$  seeps may offer testing grounds for exploring new  $p\text{CO}_2$  proxies under natural conditions at high  $p\text{CO}_2$  levels like those encountered in the geological past.

*Data availability.* All data are present in the paper and/or in the Supplement.

*Supplement.* The supplement related to this article is available online at: <https://doi.org/10.5194/bg-16-4451-2019-supplement>.

*Author contributions.* CRW, SS, and JSSD designed the study. SA, BPH, and CRW collected field samples. CRW analyzed samples and wrote the manuscript. CRW, MTJvdM, JSSD, and SS interpreted the data.

*Competing interests.* The authors declare that they have no conflict of interest.

*Acknowledgements.* We thank Jason M. Hall-Spencer, Marco Milazzo, and Yasutaka Tsuchiya for their help in sample collection. We also thank Jort Ossebaar and Ronald van Bommel at the NIOZ for technical support. This study received funding from the Netherlands Earth System Science Center (NESSC) through a gravitation grant (024.002.001) to Jaap S. Sinninghe Damsté and Stefan Schouten from the Dutch Ministry for Education, Culture, and Science.

*Financial support.* This research has been supported by the Netherlands Earth Systems Science Center (grant no. 024.002.001).

*Review statement.* This paper was edited by Clare Woulds and reviewed by three anonymous referees.

## References

- Agostini, S., Wada, S., Kon, K., Omori, A., Kohtsuka, H., Fujimura, H., Tsuchiya, Y., Sato, T., Shinagawa, H., Yamada, Y., and Inaba, K.: Geochemistry of two shallow  $\text{CO}_2$  seeps in Shikine Island (Japan) and their potential for ocean acidification research, *Regional Studies in Marine Science*, 2, 45–53, 2015.
- Agostini, S., Harvey, B. P., Wada, S., Kon, K., Milazzo, M., Inaba, K., and Hall-Spencer, J. M.: Ocean acidification drives community shifts towards simplified non-calcified habitats in a subtropical-temperate transition zone, *Sci. Rep.*, 8, 11354, <https://doi.org/10.1038/s41598-018-29251-7>, 2018.
- Badger, M. P. S., Chalk, T. B., Foster, G. L., Bown, P. R., Gibbs, S. J., Sexton, P. F., Schmidt, D. N., Pälke, H., Mackensen, A., and Pancost, R. D.: Insensitivity of alkenone carbon isotopes to atmospheric  $\text{CO}_2$  at low to moderate  $\text{CO}_2$  levels, *Clim. Past*, 15, 539–554, <https://doi.org/10.5194/cp-15-539-2019>, 2019.
- Benthien, A., Zondervan, I., Engel, A., Hefter, J., Terbruggen, A., and Riebesell, U.: Carbon isotopic fractionation during a mesocosm bloom experiment dominated by *Emiliania huxleyi*: Effects of  $\text{CO}_2$  concentration and primary production, *Geochim. Cosmochim. Ac.*, 71, 1528–1541, <https://doi.org/10.1016/j.gca.2006.12.015>, 2007.
- Bice, K. L., Birgel, D., Meyers, P. A., Dahl, K. A., Hinrichs, K. U., and Norris, R. D.: A multiple proxy and model study of Cretaceous upper ocean temperatures and atmospheric  $\text{CO}_2$  concentrations, *Paleoceanography*, 21, PA2002, <https://doi.org/10.1029/2005PA001203>, 2006.
- Bidigare, R. R., Fluegge, A., Freeman, K. H., Hanson, K. L., Hayes, J. M., Hollander, D., Jasper, J. P., King, L. L., Laws, E. A., Milder, J., Millero, F. J., Pancost, R., Popp, B. N., Steinberg, P. A., and Wakeham, S. G.: Consistent fractionation of C-13 in nature and in the laboratory: Growth-rate effects in some haptophyte algae, *Global Biogeochem. Cy.*, 11, 279–292, 1997.
- Boatta, F., D'Alessandro, W., Gagliano, A. L., Liotta, M., Milazzo, M., Rodolfo-Metalpa, R., Hall-Spencer, J. M., and Parello, F.: Geochemical survey of Levante Bay, Vulcano Island (Italy), a natural laboratory for the study of ocean acidification, *Mar. Pollut. Bull.*, 73, 485–494, 2013.
- Bowen, G. J. and Beerling, D. J.: An integrated model for soil organic carbon and  $\text{CO}_2$ : Implications for paleosol carbonate  $p\text{CO}_2$  paleobarometry, *Global Biogeochem. Cy.*, 18, GB1026, <https://doi.org/10.1029/2003gb002117>, 2004.
- Breecker, D. O., Sharp, Z. D., and McFadden, L. D.: Atmospheric  $\text{CO}_2$  concentrations during ancient greenhouse climates were similar to those predicted for AD 2100, *P. Natl. Acad. Sci. USA*, 107, 576–580, 2010.
- Brinkman, T. J. and Smith, A. M.: Effect of climate change on crustose coralline algae at a temperate vent site, White Island, New Zealand, *Mar. Freshwater Res.*, 66, 360–370, 2015.

- Castañeda, I. S., Werne, J. P., and Johnson, T. C.: Influence of climate change on algal community structure and primary productivity of Lake Malawi (East Africa) from the Last Glacial Maximum to present, *Limnol. Oceanogr.*, 54, 2431–2447, 2009.
- Cotton, J. M. and Sheldon, N. D.: New constraints on using paleosols to reconstruct atmospheric  $p\text{CO}_2$ , *Geol. Soc. Am. Bull.*, 124, 1411–1423, 2012.
- DaMatta F. M., Godoy A. G., Menezes-Silva P. E., Martins S. C., Sanglard L. M., Morais L. E., Torre-Neto, A., and Ghini, R.: Sustained enhancement of photosynthesis in coffee trees grown under free-air  $\text{CO}_2$  enrichment conditions: disentangling the contributions of stomatal, mesophyll, and biochemical limitations, *J. Exp. Bot.*, 67, 341352, <https://doi.org/10.1093/jxb/erv463>, 2016.
- Dando, P. R., Stuben, D., and Varnavas, S. P.: Hydrothermalism in the Mediterranean Sea, *Prog. Oceanogr.*, 44, 333–367, 1999.
- de Leeuw, J. W., Meer, F. W. V. D., Rijpstra, W. I. C., and Schenck, P. A.: On the occurrence and structural identification of long chain unsaturated ketones and hydrocarbons in sediments, in: *Advances in Organic Geochemistry*, edited by: Douglas, A. E. and Maxwell, J. R., Pergamon, Oxford, 211–217, 1980.
- Ellsworth, D. S., Thomas, R., Crous, K. Y., Palmroth, S., Ward, E., Maier, C., DeLucia, E. and Oren, R.: Elevated  $\text{CO}_2$  affects photosynthetic responses in canopy pine and subcanopy deciduous trees over 10 years: a synthesis from Duke FACE, *Glob. Change Biol.*, 18, 223–242, <https://doi.org/10.1111/j.1365-2486.2011.02505.x>, 2012.
- Fabricius, K. E., Langdon, C., Uthicke, S., Humphrey, C., Noonan, S., De'ath, G., Okazaki, R., Muehlehner, N., Glas, M. S., and Lough, J. M.: Losers and winners in coral reefs acclimatized to elevated carbon dioxide concentrations, *Nat. Clim. Change*, 1, 165–169, 2011.
- Farquhar, G. D., O'Leary, M. H., and Berry, J. A.: On the Relationship between Carbon Isotope Discrimination and the Inter-Cellular Carbon-Dioxide Concentration in Leaves, *Aust. J. Plant Physiol.*, 9, 121–137, 1982.
- Farquhar, G. D., Ehleringer, J. R., and Hubick, K. T.: Carbon Isotope Discrimination and Photosynthesis, *Ann. Rev. Plant Phys.*, 40, 503–537, 1989.
- Forster, P., Ramaswamy, V., Artaxo, P., Bernsten, T., Betts, R., Fahey, D. W., Haywood, J., Lean, J., Lowe, D. C., Myhre, G., Nganga, J., Prinn, R., Raga, G., Schulz, M., and Van Dorland, R.: Contribution of Working Group I to the Fourth Assessment Report of the Intergovernmental Panel on Climate Change, in: *Climate Change 2007: The Physical Science Basis*, edited by: Solomon, S., Qin, D., Manning, M., Chen, Z., Marquis, M., Averyt, K. B., Tignor, M., and Miller, H. L., Cambridge University Press, Cambridge, UK, 131–217, 2007.
- Foster, G. L., Royer, D. L., and Lunt, D. J.: Future climate forcing potentially without precedent in the last 420 million years, *Nat. Commun.*, 8, 14845, <https://doi.org/10.1038/ncomms14845>, 2017.
- Francois, R., Altabet, M. A., Goericke, R., McCorkle, D. C., Brunet, C., and Poisson, A.: Changes in the Delta-C-13 of Surface-Water Particulate Organic-Matter across the Subtropical Convergence in the Sw Indian-Ocean, *Global Biogeochem. Cy.*, 7, 627–644, 1993.
- Freeman, K. H. and Hayes, J. M.: Fractionation of Carbon Isotopes by Phytoplankton and Estimates of Ancient  $\text{CO}_2$  Levels, *Global Biogeochem. Cy.*, 6, 185–198, 1992.
- Goericke, R. and Fry, B.: Variations of Marine Plankton Delta-C-13 with Latitude, Temperature, and Dissolved  $\text{CO}_2$  in the World Ocean, *Global Biogeochem. Cy.*, 8, 85–90, 1994.
- Hall-Spencer, J. M., Rodolfo-Metalpa, R., Martin, S., Ransome, E., Fine, M., Turner, S. M., Rowley, S. J., Tedesco, D., and Buia, M. C.: Volcanic carbon dioxide vents show ecosystem effects of ocean acidification, *Nature*, 454, 96–99, 2008.
- Harvey, B. P., Agostini, S., Wada, S., Inaba, K., and Hall-Spencer, J. M.: Dissolution: The Achilles' Heel of the Triton Shell in an Acidifying Ocean, *Front. Mar. Sci.*, 5, 371, <https://doi.org/10.3389/fmars.2018.00371>, 2018.
- Hayes, J. M.: Factors Controlling C-13 Contents of Sedimentary Organic-Compounds – Principles and Evidence, *Mar. Geol.*, 113, 111–125, 1993.
- Hayes, J. M., Freeman, K. H., Popp, B. N., and Hoham, C. H.: Compound-Specific Isotopic Analyses – a Novel Tool for Reconstruction of Ancient Biogeochemical Processes, *Org. Geochem.*, 16, 1115–1128, 1990.
- Hayes, J. M., Strauss, H., and Kaufman, A. J.: The abundance of C-13 in marine organic matter and isotopic fractionation in the global biogeochemical cycle of carbon during the past 800 Ma, *Chem. Geol.*, 161, 103–125, 1999.
- IPCC: The Physical Science Basis, Contribution of Working Group I to the Fifth Assessment Report of the Intergovernmental Panel on Climate Change, Cambridge, ARS, 1535 pp., 2013.
- Jasper, J. P. and Hayes, J. M.: A Carbon Isotope Record of  $\text{CO}_2$  Levels during the Late Quaternary, *Nature*, 347, 462–464, 1990.
- Jasper, J. P., Hayes, J. M., Mix, A. C., and Prahl, F. G.: Photosynthetic Fractionation of C-13 and Concentrations of Dissolved  $\text{CO}_2$  in the Central Equatorial Pacific during the Last 255,000 Years, *Paleoceanography*, 9, 781–798, 1994.
- Klok, J., Cox, H. C., Deleeuw, J. W., and Schenck, P. A.: Loliolides and Dihydroactinidiolide in a Recent Marine Sediment Probably Indicate a Major Transformation Pathway of Carotenoids, *Tetrahedron Lett.*, 25, 5577–5580, 1984.
- Laws, E. A., Popp, B. N., Bidigare, R. R., Kennicutt, M. C., and Macko, S. A.: Dependence of Phytoplankton Carbon Isotopic Composition on Growth-Rate and  $[\text{CO}_2](\text{Aq})$  – Theoretical Considerations and Experimental Results, *Geochim. Cosmochim. Acta.*, 59, 1131–1138, 1995.
- Lewis, E. and Wallace, D.: Program developed for  $\text{CO}_2$  system calculations, Oak Ridge National Laboratory, Oak Ridge, Tennessee, 1998.
- Liaaen-Jensen, S.: Marine carotenoids, in: *Marine natural products*, edited by: Scheuer, P. J., Academic Press, 747–759, 1978.
- Lüthi, D., Le Floch, M., Bereiter, B., Blunier, T., Barnola, J. M., Siegenthaler, U., Raynaud, D., Jouzel, J., Fischer, H., Kawamura, K., and Stocker, T. F.: High-resolution carbon dioxide concentration record 650,000–800,000 years before present, *Nature*, 453, 379–382, 2008.
- Madigan, M. T., Takigiku, R., Lee, R. G., Gest, H., and Hayes, J. M.: Carbon Isotope Fractionation by Thermophilic Phototrophic Sulfur Bacteria – Evidence for Autotrophic Growth in Natural Populations, *Appl. Environ. Microbiol.*, 55, 639–644, 1989.
- Mook, W. G. B., Bommerson, J. C., and Staverman, W. H.: Carbon isotope fractionation between dissolved bicarbonate and gaseous carbon dioxide, *Earth Planet. Sci. Lett.*, 22, 169–176, [https://doi.org/10.1016/0012-821X\(74\)90078-8](https://doi.org/10.1016/0012-821X(74)90078-8), 1974.

- Mouritsen, O. G. and Zuckermann, M. J.: What's so special about cholesterol?, *Lipids*, 39, 1101–1113, 2004.
- Nes, W. D., Janssen, G. G., Crumley, F. G., Kalinowska, M., and Akihisa, T.: The Structural Requirements of Sterols for Membrane-Function in *Saccharomyces-Cerevisiae*, *Arch. Biochem. Biophys.*, 300, 724–733, 1993.
- Pagani, M.: The alkenone-CO<sub>2</sub> proxy and ancient atmospheric carbon dioxide, *Philos. T. R. S. S-A*, 360, 609–632, 2002.
- Popp, B. N., Takigiku, R., Hayes, J. M., Louda, J. W., and Baker, E. W.: The Post-Paleozoic Chronology and Mechanism of C-13 Depletion in Primary Marine Organic-Matter, *Am. J. Sci.*, 289, 436–454, 1989.
- Popp, B. N., Laws, E. A., Bidigare, R. R., Dore, J. E., Hanson, K. L., and Wakeham, S. G.: Effect of phytoplankton cell geometry on carbon isotopic fractionation, *Geochim. Cosmochim. Ac.*, 62, 69–77, 1998.
- Quast, A., Hoefs, J., and Paul, J.: Pedogenic carbonates as a proxy for palaeo-CO<sub>2</sub> in the Palaeozoic atmosphere, *Palaeogeogr. Palaeocl.*, 242, 110–125, <https://doi.org/10.1016/j.palaeo.2006.05.017>, 2006.
- Rau, G. H., Riebesell, U., and WolfGladrow, D.: A model of photosynthetic C-13 fractionation by marine phytoplankton based on diffusive molecular CO<sub>2</sub> uptake, *Mar. Ecol. Prog. Ser.*, 133, 275–285, 1996.
- Repeta, D. J.: Carotenoid Diagenesis in Recent Marine-Sediments, 2. Degradation of Fucoxanthin to Loliolide, *Geochim. Cosmochim. Ac.*, 53, 699–707, 1989.
- Schouten, S., Breteler, W. C. M. K., Blokker, P., Schogt, N., Rijpstra, W. I. C., Grice, K., Baas, M., and Sinninghe Damsté, J. S.: Biosynthetic effects on the stable carbon isotopic compositions of algal lipids: Implications for deciphering the carbon isotopic biomarker record, *Geochim. Cosmochim. Ac.*, 62, 1397–1406, 1998.
- Sinninghe Damsté, J. S., Kuypers, M. M. M., Pancost, R. D., and Schouten, S.: The carbon isotopic response of algae, (cyano)bacteria, archaea and higher plants to the late Cenomanian perturbation of the global carbon cycle: Insights from biomarkers in black shales from the Cape Verde Basin (DSDP Site 367), *Org. Geochem.*, 39, 1703–1718, 2008.
- Stoll, H. M., Guitian, J., Hernandez-Almeida, I., Mejia, L. M., Phelps, S., Polissar, P., Rosenthal, Y., Zhang, H. R., and Ziveri, P.: Upregulation of phytoplankton carbon concentrating mechanisms during low CO<sub>2</sub> glacial periods and implications for the phytoplankton *p*CO<sub>2</sub> proxy, *Quaternary Sci. Rev.*, 208, 1–20, <https://doi.org/10.1016/j.quascirev.2019.01.012>, 2019.
- van Bentum, E. C., Reichart, G. J., and Sinninghe Damsté, J. S.: Organic matter provenance, palaeoproductivity and bottom water anoxia during the Cenomanian/Turonian oceanic anoxic event in the Newfoundland Basin (northern proto North Atlantic Ocean), *Org. Geochem.*, 50, 11–18, 2012.
- Volkman, J. K., Eglinton, G., Corner, E. D. S., and Forsberg, T. E. V.: Long-Chain Alkenes and Alkenones in the Marine Coccolithophorid *Emiliania-Huxleyi*, *Phytochemistry*, 19, 2619–2622, 1980.
- Ward, E., Oren, R., Bell, D.M., Clark, J.S., McCarthy, H.R., Kim, H.-S., and Domec, J.-C.: The effects of elevated CO<sub>2</sub> and nitrogen fertilization on stomatal conductance estimated from 11 years of scaled sap flux measurements at Duke FACE, *Tree Physiol.*, 33, 2, 135151, <https://doi.org/10.1093/treephys/tps118>, 2013.
- Wei, J. H., Yin, X. C., and Welandar, P. V.: Sterol Synthesis in Diverse Bacteria, *Front. Microbiol.*, 7, 990, <https://doi.org/10.3389/fmicb.2016.00990>, 2016.
- Weiss, R. F.: Carbon dioxide in water and seawater: The solubility of a non-deal gas, *Mar. Chem.*, 2, 203–215, [https://doi.org/10.1016/0304-4203\(74\)90015-2](https://doi.org/10.1016/0304-4203(74)90015-2), 1974.
- Witkowski, C. R., Weijers, J. W. H., Blais, B., Schouten, S., and Sinninghe Damsté, J. S.: Molecular fossils from phytoplankton reveal secular *p*CO<sub>2</sub> trend over the Phanerozoic, *Sci. Adv.*, 4, eaat4556, <https://doi.org/10.1126/sciadv.aat4556>, 2018.
- Xu, Z., Jiang, Y., Jia, B., and Zhou, G.: Elevated-CO<sub>2</sub> response of stomata and its dependence on environmental factors, *Front. Plant Sci.*, 7, 657, <https://doi.org/10.3389/fpls.2016.00657>, 2016.
- Zhang, Y. G., Pagani, M., Liu, Z. H., Bohaty, S. M., and DeConto, R.: A 40-million-year history of atmospheric CO<sub>2</sub>, *Philos. T. R. Soc. A*, 7, 371, <https://doi.org/10.1098/rsta.2013.0096>, 2013.